

## Implementation of a fixed-location time lapse photogrammetric rock slope monitoring system in Castellfollit de la Roca, Spain

Gerard Matas<sup>1</sup>, Albert Prades<sup>2</sup>, M. Amparo Núñez-Andrés<sup>2</sup>, Felipe Buill<sup>2</sup>, Nieves Lantada<sup>1</sup>

<sup>1</sup> Department of Civil and Environmental Engineering, Universitat Politècnica de Catalunya, C/ Jordi Girona 1-3, 08034 Barcelona, Spain, ([gerard.matas@upc.edu](mailto:gerard.matas@upc.edu); [nieves.lantada@upc.edu](mailto:nieves.lantada@upc.edu))

<sup>2</sup> Department of Civil and Environmental Engineering, Universitat Politècnica de Catalunya, Av. Doctor Marañón 44-50, 08028 Barcelona, Spain, ([alberto.prades.i@upc.edu](mailto:alberto.prades.i@upc.edu); [m.amparo.nunez@upc.edu](mailto:m.amparo.nunez@upc.edu); [felipe.buill@upc.edu](mailto:felipe.buill@upc.edu))

**Key words:** rockfall; time-lapse photogrammetry; monitoring; automation

### ABSTRACT

When monitoring deformations in natural hazards such as rockfalls and landslides, the use of 3D models has become a standard. Several geomatic techniques allow the generation of these models. However, each one has its pros and cons regarding accuracy, cost, sample frequency, etc. In this contribution a fixed-location time lapse camera system for continuous rockfall monitoring using photogrammetry has been developed as an alternative to Light Detection and Ranging (LiDAR) and ground-based interferometric synthetic-aperture radar (GB-InSAR). The usage of stereo photogrammetry allows the obtention of 3D points clouds at a low cost and with a high sample frequency, essential to detect premonitory displacements. In this work the designed system consists of three digital single-lens reflex (DSLR) cameras which collect photographs of the rock slope daily controlled by a Raspberry Pi computer using the open-source library gPhoto2. Photographs are automatically uploaded to a server using 3G network for processing. This system was implemented at Castellfollit de la Roca village (Girona province, Spain), which sits on a basaltic cliff that has shown significant rockfall intensity in recent years. The 3D models obtained will allow monitoring rockfalls frequency, premonitory displacements, and calculate the erosion rate of the slope. All technical decisions taken for the design and implementation on this specific site are discussed and first results shown.

### I. INTRODUCTION

In recent years, technological improvements in remote sensing technologies led to improve the characterization and monitoring of rock slope hazards and other geomorphic processes. Most used technologies for this purpose are terrestrial laser scanning (TLS), structure from motion (SfM) photogrammetry and Ground-based Interferometric synthetic-aperture radar (GB-InSAR). These three methodologies can be used in very different situations depending on the site and the required sampling frequency. GB-InSAR achieves sub-millimeter measurements of displacements for landslides at near-real time (Atzeni *et al.*, 2015). However, the high costs of GB-InSAR systems pushed the usage of TLS and SfM as cheaper and feasible alternatives. In both cases, the systems can be classified depending on the mobility and the sampling frequency. They can be mounted on fixed locations or on moving vehicles like drones or satellites and capture information at specific time intervals in an almost continuous mode or at specific moments corresponding to field campaigns. Several authors have used SfM to monitor displacements in landslides and rockfall prone areas both using fixed location cameras (Kromer *et al.*, 2019; Blanch *et al.*, 2021) or moving cameras mounted on drones (Sarro *et al.*, 2018). In the case of laser scanners most take information from the

ground since the usage of laser scanners mounted on drones is still not common. Some authors have compared SfM with TLS and concluded that each one has its strengths that may depend on the specific study site (Núñez-Andrés *et al.*, 2019).

In the specific field of rockfall monitoring and management, the three-dimensional models obtained with all these techniques are used to identify potential rockfall sources (Albarelli *et al.*, 2021), monitoring displacements to predict future events (Janeras *et al.*, 2016) and quantifying rockfall activity for obtaining magnitude frequency curves (Williams *et al.*, 2018).

In this study we present an implementation on a fixed location set of cameras in Castellfollit de la Roca study site. The objective was to develop a system able to detect precursory displacements and monitor activity for inventorying purposes. The characteristics of the study site required placing the cameras at distances around 170 meters, which is substantially higher than in other studies (Kromer *et al.*, 2019; Blanch *et al.*, 2021).

### II. STUDY SITE

The study area is in the village of Castellfollit de la Roca (Catalunya, Spain). It is located at an altitude of 296 m and sits on a basaltic cliff that is more than 50 m high and almost one kilometer long. This basaltic cliff is the consequence of the erosive action of the rivers

Fluvià and Toronell on the volcanic remains resulting from the superposition of two lava flows that are estimated to be 217.000 and 192.000 years old, respectively. On this cliff the prism shaped disjunctions that are formed when the basalt cools slowly and at rest are present. Due to erosion these basalt towers can collapse generally following a toppling failure. Previous observations with TLS (Terrestrial Laser System) detected precursory deformation of the rockfall (Abellan *et al.*, 2009; 2011). They followed an apparent stationary stage with displacements lower than 1.64 cm/year.

Contrary to the usual rockfall risk scenario in which the element exposed at risk is under the cliff, in this case it is over the cliff. The erosion of the massif on which the town is built can put at risk the buildings that are closer to it. From all the massif a specific area to monitor was chosen considering the more active part of the cliff from previous event inventories and the closest part of the cliff to the buildings.

### III. SYSTEM DESIGN AND IMPLEMENTATION

The implementation of a fixed photogrammetric camera system depends on both the site and the nature of the phenomenon under study. There are several important factors influencing the results. On the one hand the optical characteristics of the cameras (Gance *et al.*, 2014): the resolution of the cameras, the lens used and their focal length, on the other hand factors related to the system configuration: the number of cameras, the relation base/object, *i.e.* distance among cameras, and from the camera network to the target, site access constraints and environmental constraints. On the other hand, the technical requirements if the images need to be transferred remotely: the possibility of accessing the electrical connection or not, the 3G/4G signal for internet connection, the desired monitoring interval etc. (Kromer *et al.*, 2019).

The following subsections describe the solution adopted at Castellfollit de la Roca site for rockfall monitoring using a time lapse system considering all cited factors.

#### A. System components

The objective of the system is to take pictures at a regular interval for a continuous monitoring of the studied cliff. These pictures must be sent over the internet to a storage server for further processing. Since mounted outdoors, the system must withstand inclement weather. The system was placed near a populated area and thus all components could be connected to the local power grid. This simplifies the continuous use of the system since the use of solar panels and batteries was not required. The system consists of a power management unit, a control unit, a total of three cameras.

The power management unit has an electrical transformer to filter possible electrical spikes and a

surge protection system to protect all components. It is enclosed in an IP67 cage to ensure water protection. The protected cable is directly connected to the main control unit.

The control unit (Figure 1) is in charge of controlling the cameras and sending collected pictures over a 3G network to a server. The brain of the control unit is a Raspberry Pi 4 (RPi4) microcomputer, which is capable of interfacing through USB protocol with the cameras and has a Rj45 connector for internet connectivity. To allow the usage of just one microcomputer on the system, all three cameras were directly wired to the Raspberry Pi through USB. However, since the maximum allowed cable distance for USB protocol is 10 m and the two cameras were placed at more than 30 m distance from the control unit, a USB extension through ethernet was required. A relay board connected to the RPi4 is in charge of controlling the camera power supply and thus when they are turned on or turned off. To allow multiple USB connections a USB hub was plugged into the RPi4, and finally, for internet connection a 3G router was directly connected to the Rj45 port of the RPi4.

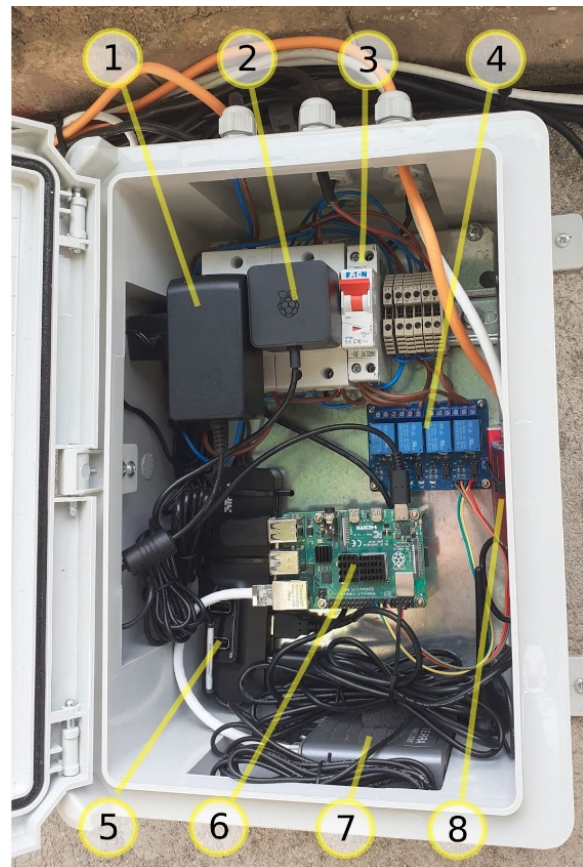


Figure 1. Control unit and its components: 1) Router power supply; 2) RPi4 Power supply; 3) Main power switch; 4) Relay board; 5) USB Hub; 6) RPi4 microcomputer; 7) 3G router; 8) USB extenders through ethernet.

Each DSLR camera is housed in a commercial protective housing used for camera trap photography. Both the camera power adapter and the USB extender receiver including its own power supply were fitted

inside the housing. Figure 2 shows the camera housing and its components. The camera that is placed next to the control unit lacks the USB extender since the distance is short enough to be covered by a single USB cable.

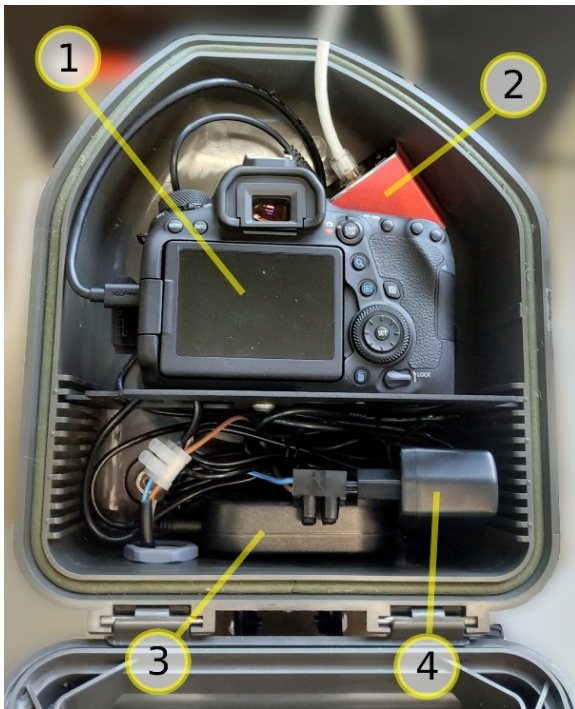


Figure 2. Single camera housing: 1) DSLR camera; 2) USB extender through ethernet receiver; 3) DSLR camera power supply; 4) USB extender power supply.

### B. System setup

The three cameras forming the system are at an average distance from the monitored area of 170 meters. This distance is greater than other similar devices (Gance *et al.*, 2014; Kromer 2019; Blanch 2021) mounted in other studios and implies a challenge when choosing the optics of the cameras. The control unit (CU) is placed next to Camera 2 (C2) and has the ability to trigger photos from all three cameras schedule based or at user request. C1, C2 and the CU were installed on the facade of an old factory, while C3 was installed on a wooden pole that supports a telecommunications cable (Figure 3). The location of the cameras allowed a 90% overlap between the central photo of C2 and C1 & C3.

### C. Cameras and lens

The geometrical constraints of the site and the required resolution condition the choice of cameras and optics. In this project, the distance from the massif to be monitored is considerable and it has been required to use telescopic optics mounted on DSLR cameras. In rockfall photogrammetric monitoring, the higher the resolution of the used camera, the smaller the volume that the system is capable of detecting. Detecting rockfalls around 0.001 m<sup>3</sup> is a key point since they can be the prelude of bigger events. With all these considerations the cameras chosen were Canon EOS 6D

Mark II, whose characteristics are CMOS sensor, aspect ratio 3:2, image format 35.9 x 24.0 mm and maximum resolution 6240 x 4160 pixels, and a focal length of 105 mm. Fixed conditions, sensibility ISO 100 and aperture f/8, are used for the photographic capture.



Figure 3. Top: Control unit next to Camera 2 (C2). Bottom: Camera 3 (C3) placed on a telecommunication wooden pole.

The capture geometry has been defined in order to achieve the best reliability in the detection of change in the basaltic columns. In this way the base distance between the cameras are 39 and 37 meters (Figure 4) with a distance to base ratio 1:5, moreover, the photographic bases were approximately parallel to the rock wall.

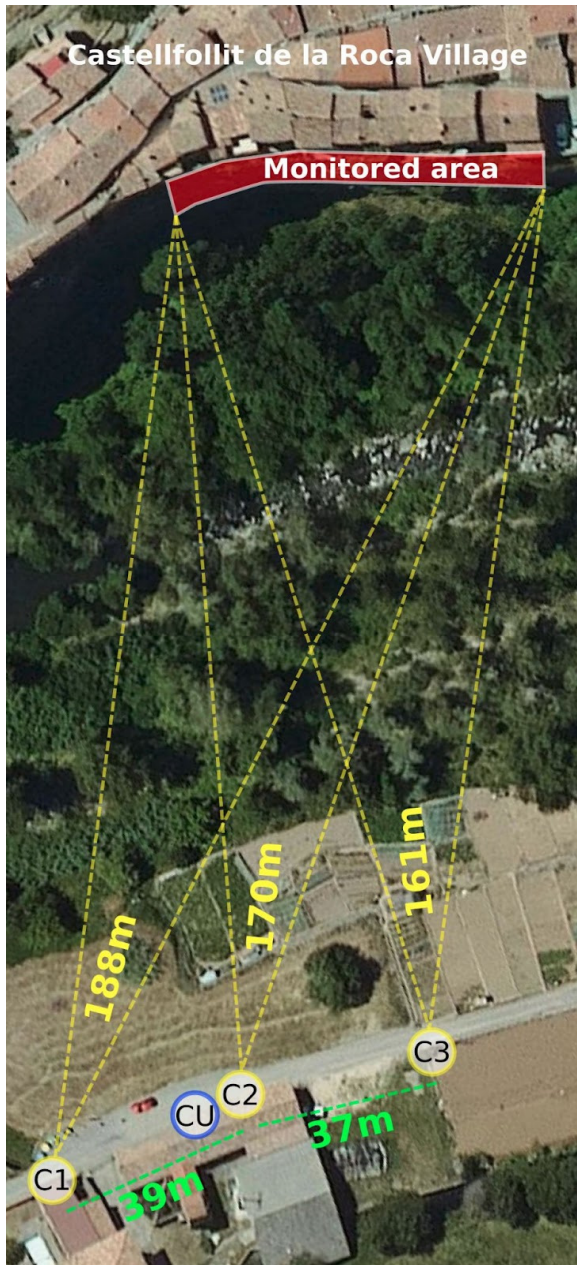


Figure 4. Position of the three cameras of the system (C1, C2 and C3) and the control unit (CU) with respect to the monitored area behind Castellfollit de la Roca village.

Through the scale ratio, Equation 1 and parallax equations, Equation 2, we calculate the minimum measurable displacement Equation 3.

$$E = \frac{Y}{f} = \frac{B}{p} \quad (1)$$

where  $E$  = scale factor  
 $Y$  = distance from reference to observed point  
 $B$  = the photographic base  
 $p$  = parallax,  $dp = \sqrt{2}dx$   
 $f$  = focal length (Figure 5).

$$X = x \cdot E \quad Y = f \cdot E = \frac{B \cdot f}{p} \quad Z = y \cdot E \quad (2)$$

$$dX = dx \cdot E \quad dY = \frac{Y^2}{B \cdot f} dp \quad dZ = dy \cdot E \quad (3)$$

where  $X, Y, Z$  = ground coordinates (GC)  
 $x, y$  = image coordinates  
 $dX, dY, dZ$  = estimated error in GC  
 $dx, dy, dz$  = distance from reference

In the worst-case scenario where cameras C1 or C3 fail, the photographic base will be  $B \approx 37$  m,  $f = 105$  mm,  $Y \approx 170$  m, and the appreciation,  $dx$  and  $dy$ , will stay within a range from  $\frac{1}{4}$  to  $\frac{1}{2}$  px. The measurable movements are  $dX \approx 0.3$  cm,  $dY \approx 1.5$  cm,  $dZ \approx 0.3$  cm, and  $dX \approx 0.6$  cm,  $dY \approx 3$  cm,  $dZ \approx 0.6$  cm considering an appreciation of  $\frac{1}{4}$  px and  $\frac{1}{2}$  px respectively. These values would be achieved in optimal conditions, however in the study area environmental humidity and changes in the temperature will affect the quality of the images and therefore the real values will be higher than the optimal ones.

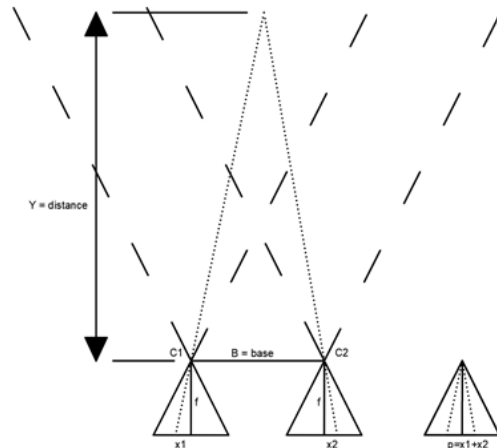


Figure 5. Coordinate system parallel to the object, X parallel to the photographic base, Y normal to this base (depth) and Z complete the normal trihedron.

#### IV. SYSTEM WORKFLOW

The microcomputer is in charge of turning on the cameras following a certain schedule. This schedule can be easily reprogrammed, for example for taking a photo every hour or for taking photos at a certain time every day. When it is time to take the pictures, the microcomputer turns on each camera one by one through the relay plate, it waits for the camera to be detected through the USB port and then prompts the device to take the picture. Once the three photographs have been taken, with all the cameras turned off, a backup copy of the three photographs is done to a USB memory and later the same photographs are sent to an intermediate server through the SFTP protocol.

The microcomputer is always turned on since everything is connected to the power grid, however it is automatically rebooted once a week. This reboot ensures that in case some part of the control software fails, up to a week of potential data could be lost.

### A. Control unit software

The microcomputer (RPI4) runs a full linux distribution, RaspberryPi OS, which is especially designed for usage on this device. The OS allows interoperability between devices through the USB protocol, the internet through RJ45 port and all access to all required libraries to manage system operations. The main control code of the system is written in Python programming language and uses the library Gphoto2 to interface and control the DSLR cameras. When this main code is called it performs the following operations:

1. Turns on the cameras using the python gpio library to control the relay board that power the cameras.
2. Asks the cameras to take pictures using the gphoto2 library.
3. Creates a backup of all the photos in the external USB memory stick.
4. Sends the photos to a server through the SFTP protocol using python sftp library.

To control when this program is triggered a linux crontab file is used which allows to specify certain triggering times during the day.

For remote control of the system it is connected to a virtual VPN provided by Zerotier service. This is required since the mobile network provider operates using a CGNAT router which masks the ip of its connected devices thus not allowing direct connection from the internet. With this virtual VPN, access to the RPI4 microcomputer is allowed through the ssh protocol as if it were connected to the local network. Having constant remote access to the system allows for tweaking of the parameters and controlling the real time performance.

### B. Data management and backups

All photos taken by the system are stored on the SD card in the RPi and on a USB stick. This allows for redundancy in case the system gets disconnected from the internet. This storage is limited and old photos must be deleted to ensure new ones have enough space. After taking and storing the photos the system sends them to an intermediate university server using SFTP. All files contained in this server are then backed up into another machine to ensure no data loss in case of a hard disk failure.

### C. Image processing

We have worked with the images in a double process. On one hand, the comparison of monoscopic images, and on the other hand the construction of the 3d model.

Since the displacement can be slow we compare the data daily, biweekly and monthly. The phases for the monoscopic imaging process are:

1. Correction of sensor movements. The cameras suffer small movements due to the wind, temperature changes etc.
2. Radiometric adjustment. However, according to Desrues *et al.*, (2019) it is not determinant.
3. Multitemporal images comparison for each camera.

## V. SYSTEM PERFORMANCE AND FIRST RESULTS

After setting up the system it has been continuously sending photographs to the server for half a year by the time of submitting this contribution. We observed that the quality of the images significantly depends on the hour at which they are taken. The sun incidence produces a blurred image because of the protective case glass. Thus, the best quality images are the ones taken at the sunset and sunrise.

The color of the basalt rock depends on the incidence of sunlight, and considerable color changes have been observed in images due to this effect.

It has been observed that the vegetation present in the study cliff is of rapid growth, making the direct comparison of images and models difficult, thus requiring a meticulous filtering process.

During this period of time the system has been working, no rockfalls have been detected on the cliff. However, the system was able to detect the presence of a bastide in a facade restoration work, as shown in Figure 6. In this figure the growth of the vegetation can also be observed (orange-red colors).

## VI. CONCLUSIONS

The implementation of time-lapse fixed position systems with DSLR cameras, using currently available open source hardware and software, has been easy and inexpensive.

These systems can work even at great distances using the right optics for the cameras. The incidence of the light on the glass of the protective cases showed a relevant sole on the quality of the images. This effect must be considered when choosing the location of the cameras when possible.

The quality of the solution is influenced not only by the optical characteristics of the camera but also dramatically by the geometry of the cameras' position. However, to select the best places to set them is not always possible.

In places like this area where there is riparian and ivy vegetation the use of vegetation mask during the image processing is essential.

Despite the difficulties, movements on the order of centimeters can be detected on the unstable boulders of the massif.

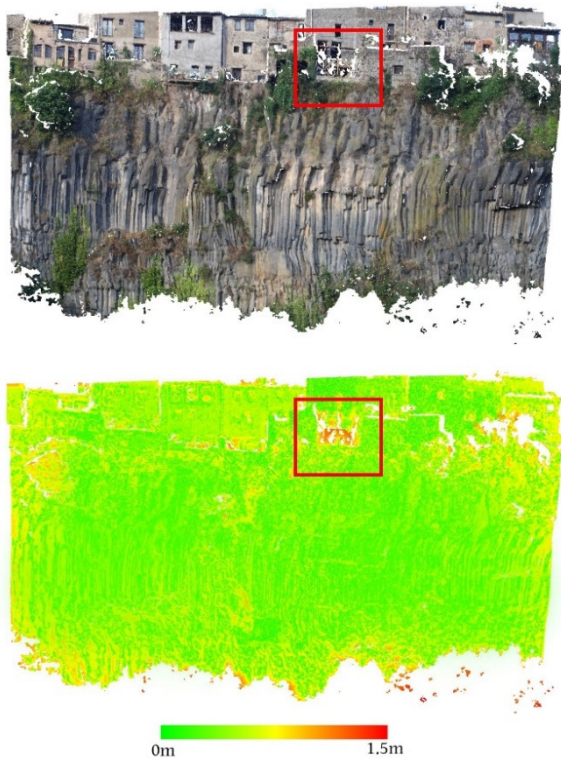


Figure 6. Cloud point comparison of two models before and after the collocation of a structure for restoring one of the buildings. Color scale shows displacement in meters.

## VII. ACKNOWLEDGEMENTS

This work has been carried within the framework of the research project Georisk “Avances en el análisis de la cuantificación del riesgo (QRA) por desprendimientos rocosos”, PID2019-103974RB-I00 funded by MCIN/AEI/10.13039/501100011033.

We want to acknowledge the ICGC team for their recommendations during the design of the system and during its implementation on the field. Also, to Vilarrasa S.L enterprise for allowing the placement of the cameras on its buildings. Finally, we appreciate all help provided by the Montagut i Oix local council.

## References

- Abellan A., Vilaplana J. M., Calvet J., García-Sellés D., and Asens E. (2011). Rockfall monitoring by Terrestrial Laser Scanning - Case study of the basaltic rock face at Castellfollit de la Roca (Catalonia, Spain). *Natural Hazards and Earth System Sciences* 11(3), pp. 829-841. DOI: 10.5194/nhess-11-829-2011
- Abellan A., Vilaplana J.M., Calvet J., and Rodríguez-Lloveras X., (2009). Detection of millimetric deformation using a terrestrial laser scanner: experiment and application to a rockfall event. *Nat. Hazards Earth Syst. Sci.*, 9, pp. 365–372. DOI: 10.5194/nhess-9-365-2009
- Albarelli, D.S.N.A., Mavrouli, O.C. and Nyktas, P. (2021). Identification of potential rockfall sources using UAV-derived point cloud. *Bull Eng Geol Environ* 80, p. 6539–6561. DOI: 10.1007/s10064-021-02306-2
- Atzeni, C., Barla, M., Pieraccini, M., and Antolini, F. (2015). Early Warning Monitoring of Natural and Engineered Slopes

with Ground-Based Synthetic-Aperture Radar. *Rock Mech. Rock Eng.*, 48, pp. 235–246.

- Blanch X., Eltner A., Guinau M. and Abellan A. (2021). Multi-Epoch and Multi-Imagery (MEMI) Photogrammetric Workflow for Enhanced Change Detection Using Time-Lapse Cameras. *Remote Sens.* 13, 1460. DOI: 10.3390/rs13081460
- Desrues, M., Malet, J.-P., Brenguier, O., Point, J., Stumpf, A., and Lorier, L. (2019). TSM—Tracing Surface Motion: A Generic Toolbox for Analyzing Ground-Based Image Time Series of Slope Deformation. *Remote Sens.*, 11, 2189. DOI: 10.3390/rs11192189
- Gance J., Malet J.-P., Dewez T., and Travelletti J. (2014). Target Detection and Tracking of moving objects for characterizing landslide displacements from time-lapse terrestrial optical images. *Engineering Geology*, 172, pp.26-40. DOI: 10.1016/j.enggeo.2014.01.003
- Janeras, M., Jara, J.A., Royán, M.J., Vilaplana, J.M., Aguasca, A., Fàbregas, X., Gili, J.A., and Buxó, P., (2016). Multi-technique approach to rockfall monitoring in the Montserrat massif (Catalonia, NE Spain), *Engineering Geology*, DOI: 10.1016/j.enggeo.2016.12.010
- Kromer, R., Walton, G., Gray, B., Lato, M., and Group, R. (2019). Development and Optimization of an Automated Fixed-Location Time Lapse Photogrammetric Rock Slope Monitoring System. *Remote Sens.*, 11, 1890. DOI: 10.3390/rs11161890
- Núñez-Andrés, M. A, Buill, F., Puig, C., Lantada, N., Prades, A., Janeras, M., and Gili, J.A. (2019). Comparison of geomatic techniques for rockfall monitoring. *4<sup>th</sup> Joint International Symposium on Deformation Monitoring (JISDM)*, 15-17 May 2019, Athens (Greece).
- Sarro, R., Riquelme, A., García-Davalillo, J.C., Mateos, R.M., Tomás, R., Pastor, J.L., Cano, M., and Herrera, G. (2018). Rockfall Simulation Based on UAV Photogrammetry Data Obtained during an Emergency Declaration: Application at a Cultural Heritage Site. *Remote Sens.*, 10, 1923. DOI: 10.3390/rs10121923
- Williams, J. G., Rosser, N. J., Hardy, R. J., Brain, M. J., and Afana, A.A. (2018). Optimising 4-D surface change detection: an approach for capturing rockfall magnitude-frequency, *Earth Surf. Dynam.*, 6, pp. 101–119, DOI: 10.5194/esurf-6-101-2018.